ASME 2014 12th Biennial Conference on Engineering Systems Design and Analysis
ESDA2014
June 25-27, 2014, Copenhagen, Denmark

ESDA2014-20067

An Investigation of the Relation Between Combustion Phase and Emissions of ULSD & RME Biodiesel with a Common-Rail HSDI Diesel Engine

Hayder A. Dhahad
Mechanical Engineering Department
University of Technology, Baghdad, Iraq

Mohammed A. Abdulhadi
Mechanical Engineering Department
University of Technology, Baghdad, Iraq

Ekhlas M. Alfayyadh
Mechanical Engineering Department
University of Technology, Baghdad, Iraq

T. Megaritis
Centre for Advanced Powertrain and Fuels Research
School of Engineering and Design, Brunel University,
London, UK

ABSTRACT

This study investigates the effect of combustion phase (premixed and diffusion phases) duration on the emissions emitted from a high speed direct injection (HSDI) diesel engine fueled with neat (100%) rapeseed methyl ester (RME) and run at a constant speed (1500 rpm) with single injection strategy at constant fuel injection pressure (800 bar) and varying fuel injection timings (-12,-9,-6,-3,0) ATDC , for two loads(2.5 and 5 bars) BMEP . The obtained results were compared with those obtained when the engine run at the same conditions but with ultra-low sulfur diesel fuel (ULSD). In-cylinder pressure was measured and analyzed using (LABVIWE) program. calculation program specially written in (MATLAB) software was used to extract the apparent heat release rate, the ignition delay, combustion duration and specify the amount of heat released during the premixed and diffusion combustion phases (premixed burn fraction PMBF) and (diffusion burn fraction DBF) . Emission measurements included; NO_x, CO, THC, CO_2 and smoke number (SN). The results showed that at high load, RME generate higher NO_x, CO and THC. Measurements and calculations indicated that ignition delay of RME was shorter than that of ULSD, which means less PMBF. This conflicting effect is probably due to the advanced start of combustion (SOC) leading to higher combustion temperature inside the combustion chamber and there will be less time available to complete the combustion. The emission results at low load showed that NO_x and CO, generated by RME were less than those generated by USLD. USLD produced soot more than RME at high load and less at low load.

1. INTRODUCTION

Biodiesel is an alternative fuel composed of fatty acid alcohol esters and produced by the transesterification of organic oils, which can be derived from any of a wide range of renewable feedstocks [1]. There is a considerable interest in biodiesel because of its domestic and renewable origin, as well as its reduced life-cycle emissions of greenhouse gas (GHG). Furthermore, there is a substantial body of evidence showing that the use of biodiesel (and biodiesel blends) has a strong and consistent beneficial effect on the emissions of hydrocarbons (HC), carbon monoxide (CO), and particulate matter (PM) [2], while the effects of biodiesel are smaller and more variable for NO_x emissions, although generally NO_x increases slightly with the use of biodiesel. The term 'NO_x' encompasses all oxides of nitrogen, but engine-out NO_x emissions are mostly comprised of NO, and the remainder is almost all NO_2, with only trace quantities of other molecules, such as N_2O [3]. The formation of NO_x occurs through several main mechanisms. In a diesel engine, the extended Zeldovich or thermal mechanism is generally considered to be dominant [4]. The thermal mechanism is a temperature dependent process; formation rates become increasingly significant past approximately 1800 K, but beneath that, they are relatively low [5]. As well as being influenced by temperature changes, thermal NO_x is dependent upon the mixture stoichiometry and high-temperature residence times [6]. Several researchers have investigated the ways in which biodiesel can affect combustion phasing, thereby influencing the NO_x emissions. The ignition delay period is related to the cetane number of the fuel, higher cetane leads to shorter ignition delay. Typically, biodiesel fuels have higher cetane numbers than petroleum diesel [7, 8] because of the absence of aromatics in biodiesel. The ignition delay ID of biodiesel varies widely depending on feedstock [9], cetane number increases with fatty acid chain length and reduced degree of unsaturation [4, 10]. A shorter ignition delay could allow the fuel mixture and initial combustion products to have a longer residence time at elevated temperature, thereby increasing the thermal NOx formation [11]. During the pre-mixed combustion period, fuel

and air that have already mixed ignite, causing a rapid rise in temperature and pressure. The extent to which these temperature and pressure increases occur depends upon the amount of fuel that has already been injected, which is related to the length of the ignition delay. The effects of biodiesel fuel on the phasing of combustion events and how this impacts the NOx emissions have been studied by many researchers [6, 12-17]. The main focus of this work was to investigate the effects of combustion phases on the emissions of a high speed direct injection (HSDI) diesel engine fueled with ultra-low sulfur diesel fuel and neat(100%) rapeseed methyl ester (RME) and run at constant speed (1500 rpm) with single injection strategy at constant fuel injection pressure (800 bar) ,with changing the injection timing (-12,-9,-6,-3,0) ATDC and loads (40N.m=2.5 bar BMEP and 80N.m=5 bar BMEP) .

2. METHODOLGY

2.1. EXPERIMENTAL SETUP

Experiments were carried out in a 2.0 lt, 4 cylinders, 16 valves, and compression ratio18.2, direct Injection Ford's Duratorq (Puma) Euro3 diesel engine. The engine was supplied by Ford as a prototype production unit which powered Ford Transits and Mondeo cars. The engine is fully instrumented and coupled to a Schenck eddy current dynamometer. The schematic of the experimental setup is shown in Figure (1). In this investigation, the engine was operated under naturally aspirated mode without EGR. Instrumentation enables the measurement of in-cylinder pressure and exhaust gas emissions under steady-state engine operating conditions. The in-cylinder pressures were measured using a Kistler pressure transducer fitted into the first cylinder of the engine. The signal from pressure transducer was amplified by the charge amplified and then recorded by the (LabView) software in conjunction with the shaft encoder. In-cylinder pressure data were collected over 100 engine cycles per measurement, and the measurement was repeated 5 times for each point in the experimental matrix .These data were averaged from 100 cycles.

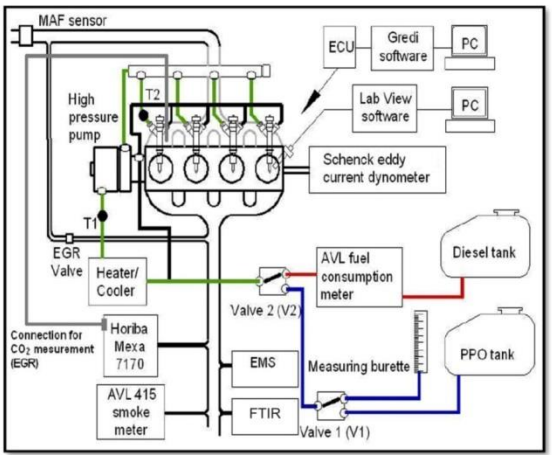

Figure1. The schematic of experimental setup

A common rail fuel injection system with six holes injector of 0.154 mm in diameter, and a spray-hole angle of 154^0 was used in this investigation. In this work, the influence of injection timing has been tested. A software (Gredi) was used to control and change engine running parameters by programming the ECU in real time. Injection timing could be directly controlled through the software. The gaseous exhaust emissions were acquired using a Horiba-Mexa 7170DEGR gas analyzer. A non-dispersive infrared method has been used for measuring the CO and CO_2 emissions. The NO_x emissions were measured using chemiluminescence technique, whereas the total un-burnt hydrocarbons (THC) were measured using the flame ionization detection technique. The engine exhaust smoke emissions were measured using the AVL – 415 smoke meter. The diesel fuel consumption was measured using an AVL fuel consumption meter, which is based on gravimetric measurement principle, measurements were carried out using the standard low sulphur diesel fuel USLD and pure rapeseed methyl ester (RME) was provided by Shell Global Solutions. Table 1 presents the properties of the fuels used in this work. NO_x composite (NO, NO_2 and N_2O) was measured using a Multigas 2030 FTIR (Fourier Transform Infrared Spectrometry) spectrometer was adopted for all emission, this unit was coupled with a FLS01 sampling device. Both units were supplied and installed by MKS Instruments UK Ltd. The FTIR instrument was cooled via liquid nitrogen supplied by BOC Specialty Gases Ltd.

Table1.
Fuel properties

Fuel analysis	**Diesel (ULSD)**	**Biodiesel (RME)**
Chemical formula	$C_{14}H_{26.18}$	$C_{18.96}H_{35.29}O_2$
Cetane number	53.9	54.7
Density at 15°C (kg/m3)	827.1	882.54
Viscosity at 40 °C (cSt)	2.467	4.478
LCV (MJ/kg)	43.3	37.4
Sulphur (mg/kg)	10	5
Total aromatics (wt%)	24.4	-
C (wt%)	86.44	77.12
H (wt%)	13.56	12.04
O (wt%)	0	10.84

2.2 Analyzing gathered data:

The data obtained from the experiments conducted were collected from relevant sensing setup using the instrumentation automation software package (LabView). Data batches collected were migrated to (Matlab) in order to process the data to obtain related values for peak pressure and the accompanying angle at which peak pressure occurred, the angle between start of combustion (SOC) and peak pressure, and to estimate the amount of apparent heat release rate (AHRR). The mathematical processing was carried out using an elementary methodology using the conventional first law heat release model assuming a constant specific heat ratio of 1.35 without any accompanying modeling of heat transfer or crevice effects. While this method was very elementary but was found to be adequate for conducting comparisons. For the purpose of ensuring that a constant value c_p/c_v could represent both fuels satisfactorily, an approximation of the c_p/c_v values made from the charts of logarithm of pressure / logarithm of volume were used in the conducted calculations. The resulting values of specific heat came out to be fundamentally consistent between ULSD and RME under different conditions. This has proven that the constant specific heat ratio used was very suitable for the purpose intended. Figure (2)

demonstrates the definitions upon which the AHHR parameters calculations were based. For the purpose of reducing noise effect on the obtained results and maintaining the crucial characteristics of combustion, each pressure point on the trace was calculated from averaging every 100 cycle pressure data. The data acquisition system logged pressure data once for every degree of crank angle, but these data were interpolated to one decimal place by a program written to run under (Matlab) .The combustion criteria parameters listed in the points after the following paragraph were calculated using the AHRR curve of figure (2) without any filtering or averaging except for the end of combustion value and the end of premixed burn. The end of combustion value was outlined using the moving average of the AHRR for the purpose of improving its consistency. The end of premixed burn was calculated from the second derivative of the AHRR. The following points list the combustion criteria calculated from the AHRR curve:

1. Start of injection (SOI): this factor was defined from the instructed SOI set within the engine management software. Any impending difference between the instructed and actual SOI is possible due to solenoid delay and should be uniform in conducted measurements as the engine speed was maintained constant.

2. Ignition delay (ID): the value of ID is defined as the difference between the instructed SOI and calculated SOC.

3. Start of combustion (SOC): the start of combustion is defined as the point at which the heat release rate becomes positive. On the AHRR curve, it is defined as the point where the curve crosses the x-axis.

4. Premixed burn Fraction (PMBF): the value for this factor is calculated from dividing the Integral of the AHRR curve between SOC and EOPMB by the Integral of the AHRR curve between SOC and EOC.

5. End of premix burn (EOPMB): the end of premix burn is defined as the first point at which the second derivative of the AHRR reaches a local maximum following a global minimum. In most conditions, the value of this factor approximates the one that corresponds to the position at which the AHRR curve reaches its first local minimum after a global maximum. But in this study, the second differential was used instead due to the reason of unclear local minimum in the AHRR curve under low load conditions which can be observed in figure (2).

6. End of combustion (EOC): this point can be defined as the first point at which the moving average of heat release rate drops below zero. The moving average was used to minimize the noise impact on the results accuracy while keeping its representative consistency with the general tendencies of collected data. Additional characteristic values can be calculated from the in-cylinder pressure data, these include: the total apparent heat release, peak AHRR, angle of peak AHRR, angle between SOC and peak AHRR, PMBF, 10 – 90% burn fraction intervals, duration of partial burn fraction intervals, and average burn rates through partial intervals. Emissions data averaged over 180 s durations were recorded.

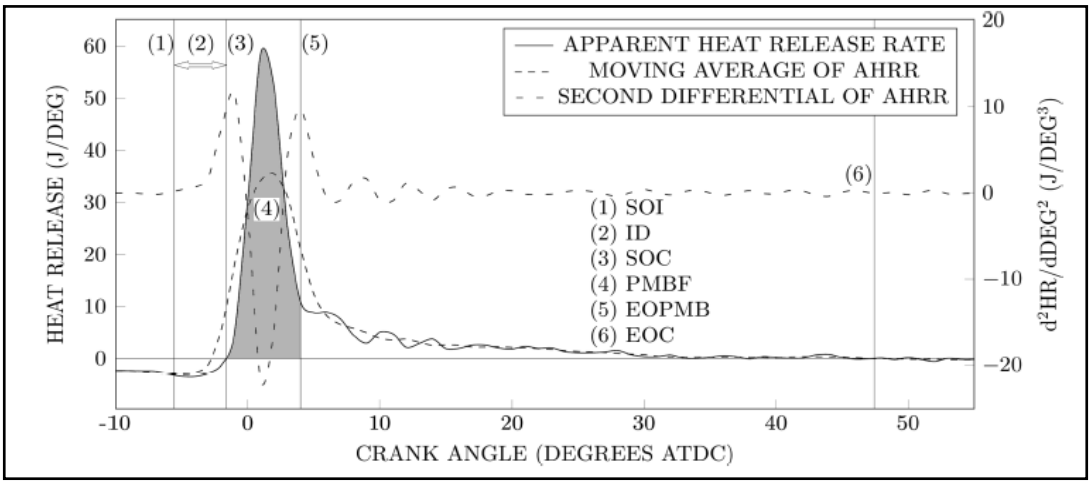

Figure (2) Labeled plot of heat release and the derivatives used to calculate combustion criteria

3. RESLUTS AND DISCUSSION

3.1 Combustion characteristics

Figure (3) shows the variations of the in-cylinder pressure with crank angle at both high and low loads (80 N.m= 5 bar BMEP & 40N.m=2.5 bar BMEP) and injection timing (-9 ATDC) for RME and USLD fuels. We can clearly note that the RME pressure curve rises earlier for both loads, but they are advanced to a slightly greater degree under the high load.

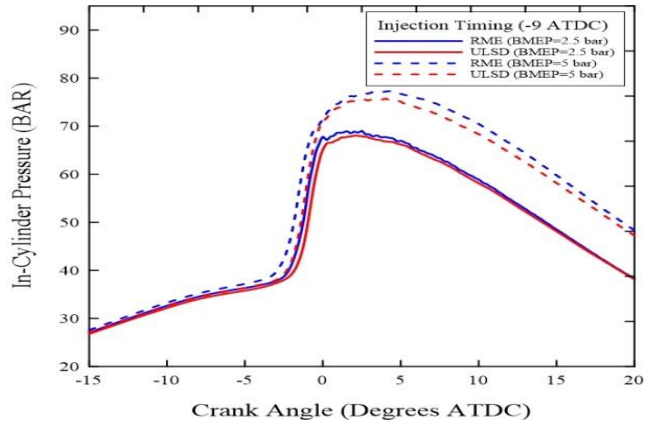

Figure (3) In-cylinder pressure at injection timing (-9ATDC) under high and low loads

This confirmation is supported by the heat release plots depicted in Figure (4) which show the same trend, and by the ID data presented in Figure (5), it is indicated that the ID of RME was always shorter than that of ULSD. The shorter ID of biodiesel is due to physicochemical properties of biodiesel (its higher viscosity, density, heat capacity, and surface tension, reduced vapor pressure, etc., which make the fuel generally more resistant to vaporization). The ignition delay also strongly depends on the cetane number of the fuel, and as the cetane number increases, the ignition delay decreases. In addition, the absence of aromatics in biodiesel increases the cetane number of biodiesel, where aromatics have low cetane numbers [18], contributing the typical longer ignition delay (ID) of petrodiesel when compared to biodiesel. On the other hand, when operating temperatures are higher (as they are at higher load), vaporization of biodiesel will occur more readily than at lower temperatures, reducing the physical component of ID time [19] . Therefore, it is probable that the larger observed reduction in ID at higher load is related to the impact of temperature change upon the physicochemical properties of biodiesel. Ignition delay decreases with the retardation of the injection timing and then returns to increase at injection timing (0 ATDC) as shown in figure (5), this is due to effect of low temperature combustion at late injection conditions.

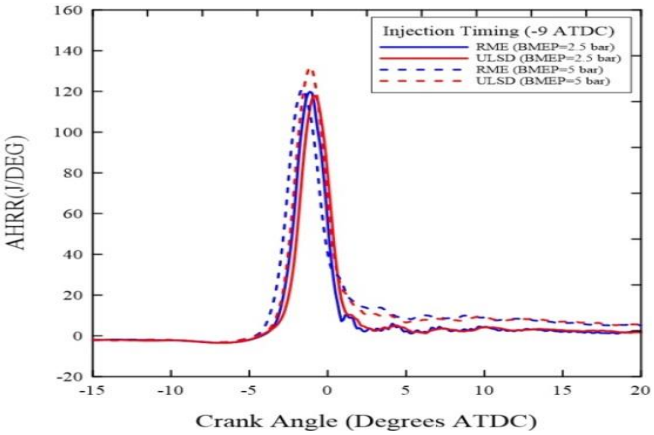

Figure (4) Apparent heat release rate at injection timing (-9ATDC) under high and low loads

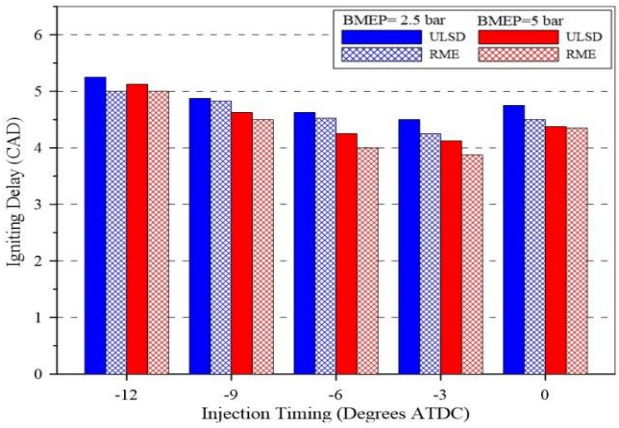

Figure (5) Ignition delay at different injection timings

The peaks of in-cylinder pressure at different injection timing are shown in Figure (6), it shows clearly that the peaks of in-cylinder pressure are mostly higher for RME.

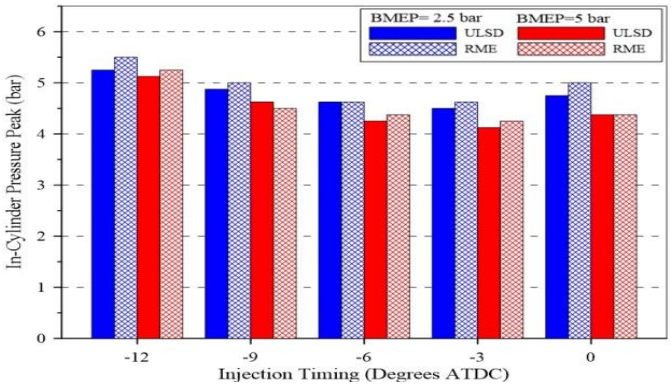

Figure (6) The peaks of in-cylinder pressure at different injection timings

This is due to the advancement of start of combustion with RME. The shorter ID of RME leads to reduce the premixed burn fraction compared to ULSD fuel as shown in Figure (7). It can be seen that premixed burn fraction decreases with the increasing of load and increasing of diffusion burn fraction, this is due to the increased amount of fuel burned during diffusion combustion. Duration of diffusion combustion increase with increasing of load, as shown in Figure (8) . The premixed and diffusion combustion duration are distinguished by using the second differential of the heat release rate, a significant difference in diffusion combustion duration between high and low loads was noticed , while there are no noticeable differences between the premixed combustion duration at both loads, Although the premixed burn duration was shorter, the magnitude of heat that is released during this phase (mass burn fraction) is higher compared to the magnitude of heat that is released in the diffusion phase ,Figure (7). This is a result of the complete combustion of premixed fuel –air mixture, also, a higher oxygen concentration in the spray will result in a reduction in pyrolysis and an increase in oxidation, which shortening the combustion duration. In Figure (7), it can be seen that at all tested conditions, the premixed burn fraction PMBF was lower for RME than for ULSD. It is also clear that PMBF values are

increasing toward advancing and retarding injection timing positions, these trends are related to ID.

The Brake Specific Fuel Consumption (BSFC) for ULSD and RME fuels at different injection timings are shown in figure (9). The BSFC for RME was higher than that of ULSD at both loads; Lapuerta et al. [20] summarized that about 98% of the researchers they had reviewed reported the increase of BSFC when using biodiesel. The increase in BSFC is mainly associated with the lower heat value of biodiesel compared with that of ULSD. The increase in BSFC at low load is a result of the incomplete combustion of fuel.

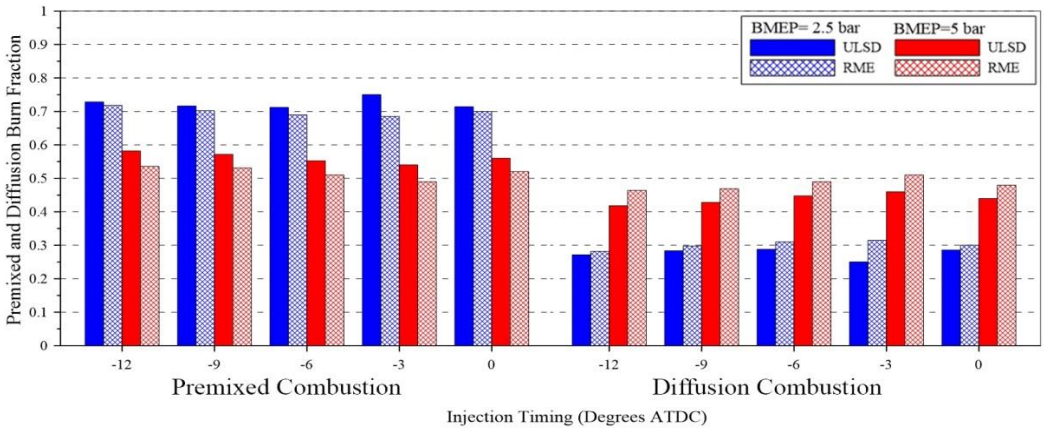

Figure (7) Effect of fuel type, injection timing and load on premixed and diffusion burn fraction

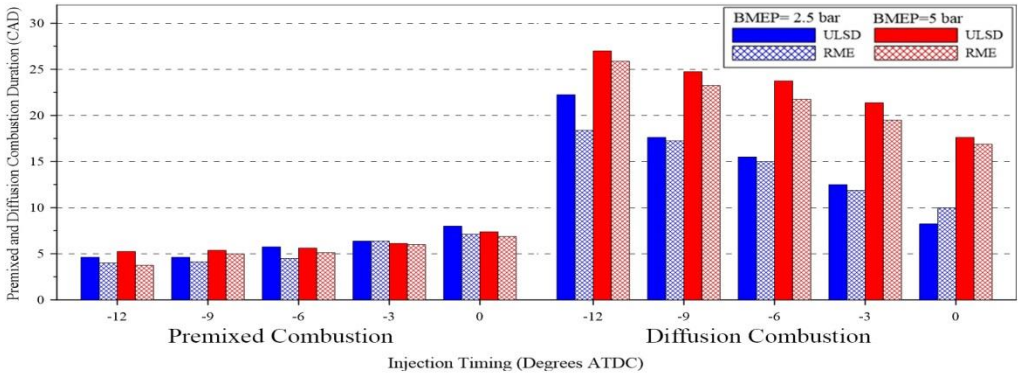

Figure (8) Effect of fuel type, injection timing and load on premixed and diffusion combustion duration

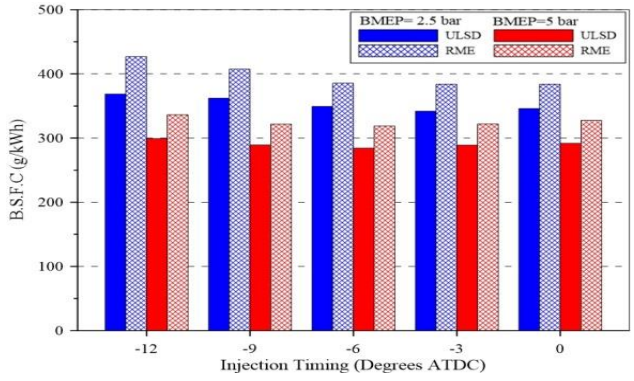

Figure (9) The Brake Specific Fuel Consumption (BSFC) at different timing

3.2 Emission characteristics

3.2.1 Nitrogen oxides

Figures (10) and (11) show the variation of (NO_x, NO, NO_2) emissions with injection timing at low and high loads, respectively. The NO_x concentration values increase with increase of engine load for both types of fuels. The reactions forming NO_x are highly temperature dependent, so the NO_x emissions have a close relation with the engine load. At low load (2.5 bar BMEP), the NO_x emissions with USLD is higher than the NO_x emissions with RME ,while at high load, the NO_x emissions with RME is higher than the NO_x emissions with USLD. Under most operational conditions, the fuel that combusted most quickly, releasing heat earliest, was the fuel that generated the highest NO_x emissions [6]. At low load ULSD had a longer ignition delay (ID) and a larger premixed burn fraction (PMBF), this will lead to a higher combustion temperature then producing highest NO_x emission. But at high load with high temperature and oxygen availability with biofuel, it will lead RME to generate higher NO_x emissions. Ban-Weiss et al [4] have suggested that the NO_x increase is not driven by the Zeldovich mechanism, but instead by the fact that during combustion the double bonded molecules cause higher levels of certain hydrocarbon radicals in the fuel rich zone of the fuel spray. This would result in an increased formation of prompt NO_x. In fuel-rich regions (the condition of high load), the oxygen content of biodiesel would

lead to an equivalence ratio relatively closer to unity, and thus a higher adiabatic flame temperature than petrodiesel under the same fuel-air mixing conditions [13, 14]. In both cases, the NO_x emissions decreases with retarded injection timings, this behavior was linked to ID and as consequence PMBF. Nearly, all NO_x emission is formed between the start of combustion and the first 20° of crank angle. Therefore, most NO_x reducing techniques are focused on this critical period [28]. Robbins et al [2] show that the effects of biodiesel usage upon NO_x emissions are small and inconsistent across all engine types, operating modes, fuel compositions, and other parameters. Figure (12) shows the NO_x emissions plotted against start of combustion SOC, which serves to demonstrate the immediate impact of RME's shorter ID. Comparing with figures (10,11) , it can be seen that NO_x emissions have same trend in all figures, this means advancing start of combustion SOC plays a critical, primary role in the increase of NO_x emissions from RME under high load .

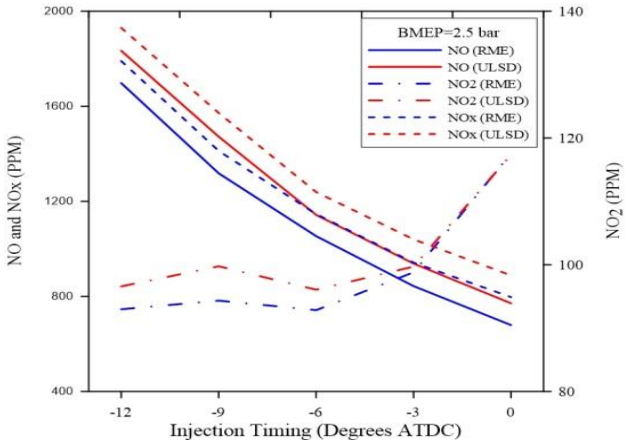

Figure (10) NOx , NO and NO2 emissions variation at low load

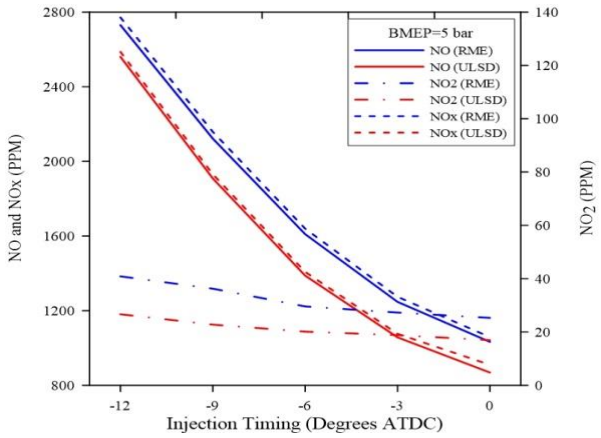

Figure (11) NOx , NO and NO2 emissions variation at high load

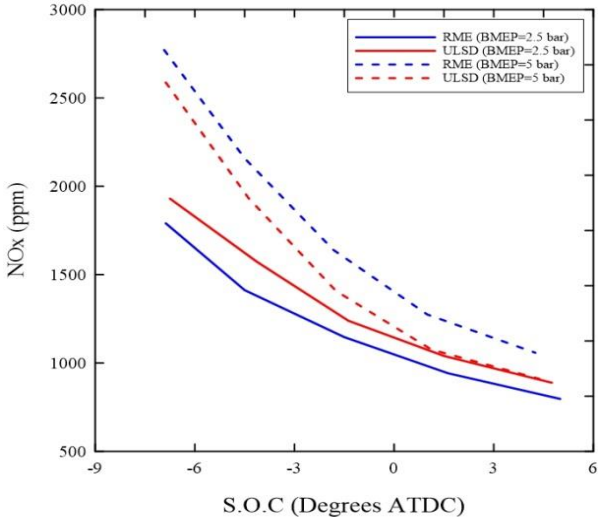

Figure (12) NOx emissions as a function of start of combustion timing under high and low loads

NO_x emissions usually include nitric oxide (NO) and nitrogen dioxide (NO_2), with NO being the predominant oxide of nitrogen produced inside the engine cylinder. NO has the same trend of NO_x , as shown in figures (10, 11). With an increase of the engine load, the percentage of NO in NO_x increases. At high load, the percentage of NO in NO_x is around 98% for both fuel types. While at low load, the percentage of NO in NO_x decrease to about (85 – 94) % with retarding injection timings for RME, and decreases to about (86-95) for ULSD . These trends are related to low combustion temperature at late combustion conditions. As a result, the percentage of NO_2 in NO_x increases with retarded injection timings at low load for both types of fuels, as shown in figure (10). Tan et al [22] showed that the biodiesel blend ratios have a little effect on the NO/NO_x ratio at middle and high engine loads. In this work, it was found that NO/NO_x ratio increases with engine load, and this illustrates that a higher temperature in the cylinder contributes to NO formation. Our results agree with Di et al [23] who find that with an increase of the engine load, the percentage of NO in NO_x increases. With the addition of biodiesel, the percentage of NO in NO_x decreases slightly. NO2 decreased with load increase. It is possible that the low load leads to lower gas temperature, and hence more NO is converted into NO_2. NO_2 is a toxic and highly reactive gas.

3.2.2 Smoke number

Figure (13) shows that the smoke emission of RME was lower than of USLD fuel, the difference is particularly obvious at high engine loads, but there is a little difference at low engine loads. The reduction of smoke number with biodiesel can be attributed to the increase of oxygen content in the fuel. The oxygen in the fuel can assist in reducing smoke formation during the stage of diffusion combustion. The improvement is more obvious at high engine loads when a larger percentage of fuel is burned in the diffusion mode, as shown in figure (7). Sooting is reduced when fuelling on biodiesel because of the oxygen content of the fuel and the chemical structure of the hydrocarbons, of which it is composed [6]. The decrease of fuel aromatics of the biodiesel could also lead to the reduction

of soot formation, where aromaticity in particular tends to increase the sooting tendency of a fuel, as it increase length of the hydrocarbon chain [24,25]. The absence of aromatics in biodiesel, have direct effect on soot format.

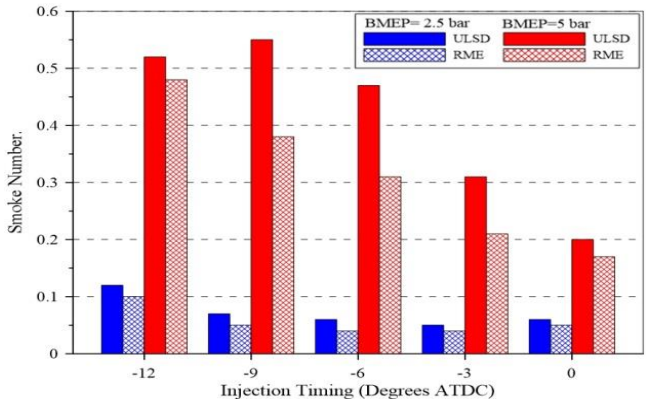

Figure (13) Effect of fuel type, injection timing and load on Smoke Number

One of the major difficulties in conventional diesel engines is the NO_x-soot trade off. Premixed combustion, during which in-cylinder pressure and temperature are very high, plays an important role in NO formation [26]. Techniques to control NO_x formation are mainly linked to a reduction in combustion temperature during this phase of combustion. Unfortunately, a reduction in combustion temperature also leads to an increase in soot emissions. The reduction in soot leads to a reduction in soot radiative heat losses; soot radiative heat losses have been identified as a significant cause of NO_x reduction when operating on traditional petrodiesel, due to the associated temperature reduction [29]. Since in-cylinder soot quantities are lower when fuelling with biodiesel, the magnitude of this temperature reduction may decline, leading to increased temperatures and higher NO_x emissions [14]. In addition to increased thermal NO_x due to a reduction in radiative heat losses, it has also been hypothesized that a reduction in soot formation may be chemically associated with increased NO_x formation via the prompt NO mechanism [30, 31]. Ban-Weiss et al [4] have shown that radiative heat transfer from soot can significantly influence NO_x formation in combustion systems. They have been reported that the "cooling effect" of soot radiation may reduce NO_x emissions by approximately 25%. For a large PMBF (at low load) , the in-cylinder soot quantities was found that low when fuelling with both ULSD and RME, and therefore the radiative heat losses would be reduced, leading to higher actual temperatures [27], and the tendency to generate lesser differences in NO_x emissions for similar combustion behavior. While, at high load when the PMBF reduced and DBF increased, the in-cylinder soot quantities would be expected to be higher for ULSD than RME, leading to increased heat losses and lower NO_x emissions when fuelling with ULSD [6].

3.2.3 CO emissions

The characteristics of CO emission are shown in Figure (14). The difference between the CO emissions at high and low loads is quite clear. The CO emissions decrease generally with increase of engine load, due to the increase of combustion temperature. CO emissions are primarily controlled by the local fuel-air equivalence ratio. In general, low local cylinder temperatures and lean fuel-air mixture regions at low engine loads may cause the combustion reactions to be unstable, so that CO can't continuously react into CO_2, the carbon monoxide concentration appears to freeze, leading to CO formation. Another reason is that, when operated with a fuel-rich equivalence ratio at high engine load, there is not enough oxygen to convert the entire carbon to carbon dioxide; as a result, some fuel does not get fully burned, and some carbon ends up emitted as CO. The molecular oxygen in biodiesel fuel improves the combustion for local rich mixtures, and the high cetane number of biodiesel fuel leads to less fuel-rich zone formation; consequently, the CO emission decreases. The effect of the retarded injection timing at low load causes higher increase of CO emissions, As mentioned above, CO emissions are formed as a result of incomplete combustion, mainly due to the combustion taking place at low temperature in the expansion stroke. Moreover, the spray-wall impingement could be much greater for the injection of fuel at TDC. This effect was not clear at high load due to the high temperature of the combustion chamber at different conditions. Robbins et al [2] show that results from light-duty engines testing are showing small increases in CO with increasing Bio-level.

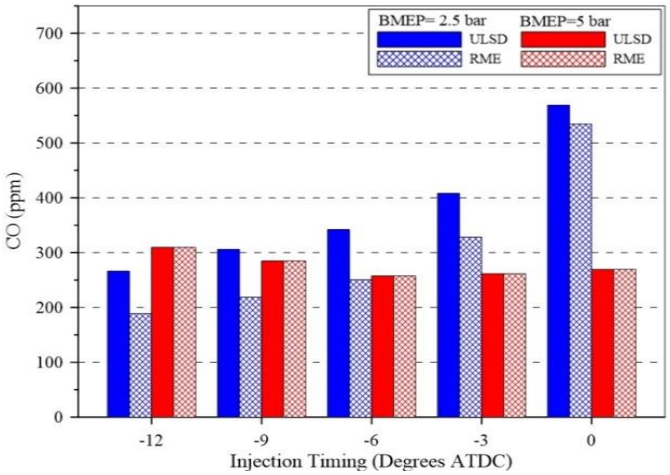

Figure (14) Effect of fuel type, injection timing and load on CO emissions

3.2.4 THC emissions

The characteristics of THC emissions are shown in Figure (15). For ULSD, the THC emission decreases with increase of engine load, due to the increase in combustion temperature associated with higher engine load. For biodiesel fuel at high load, the HC emission is higher than that of ULSD. The un-burnt hydrocarbon emissions are generally formed as a result of flame quenching , and they are strongly related to the higher viscosity of RME. Higher viscosity also leads to longer spray penetration. As a result, wetting of the cylinder walls eventually leads to the formation of higher THC emissions by incomplete combustion. THC emission can also be increased due to the presence of very lean mixture combustion (low temperature combustion) caused by over-mixing due to the

longer ignition delay period at low load. ANNEX A summarizes the emissions results of the research.

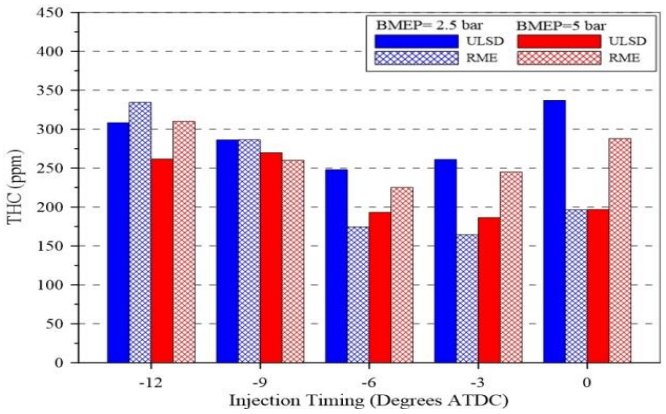

Figure (15) Effect of fuel type, injection timing and load on THC emissions

4. CONCLUSIONS

1- At all measured conditions, ULSD had a longer ID and a larger PMBF than RME. This will advance the start of combustion of RME.
2- The increased premixed burn fraction leads to an increase in temperature and thus increasing NO_x emissions and reducing soot emissions for both types of fuels. While with the increase of load, the premixed burn fraction will decrease, but NO_x and soot emissions increase due to high temperature and increase of the diffusion burn fraction, respectively.
3- The NO_x emissions from RME were lower than those from ULSD under low load, but at high load RME generated higher NO_x emissions at all injection timings.
4- The percentage of NO_2 in NO_x increases with retarded injection timings at low load for both types of fuels, due to low combustion temperature at late combustion conditions.
5- The diffusion burn fraction was large at high load for both types of fuels, which led to a significant increase of soot emissions compared to those at low load. Sooting is reduced when fuelling on biodiesel because of the oxygen content of the fuel and the chemical structure of the RME molecules.
6- For a large PMBF, the in-cylinder soot quantities appears to be low when fuelling with both types of fuels, and therefore radiative heat losses would be reduced, leading to higher actual temperatures, and the tendency to generate lesser differences in NO_x emissions for similar combustion behavior.
7- At high load when the PMBF reduced, the in-cylinder soot quantities would be expected to be higher for ULSD than RME, leading to increase heat losses and lower NO_x emissions when fuelling with ULSD.
8- (CO) and (THC) emissions are formed as a result of incomplete combustion, mainly due to the combustion taking place at low temperature in low load. This increase in CO and THC emission can also be related to the presence of very lean mixture caused by over-mixing due to the longer ignition delay period.
9- The BSFC for RME was higher than that of ULSD at both loads, due to the lower heating value of biodiesel compared with that of ULSD.

NOMENCLATURE

AHRR	Apparent heat release rate
ATDC	After top dead centre
BMAP	Brake Mean Effective Pressure
BSFC	Brake Specific Fuel Consumption
CO	Carbon monoxide
CO_2	Carbon dioxide
C_p	Specific heat at constant pressure
C_v	Specific heat at constant volume
DBF	Diffusion burn fraction
ECU	Electronic Control Unit
EGR	Exhaust Gas Recirculation
EOC	End of combustion
EOPMB	End of premixed burn
HSDI	High speed direct injection
ID	Ignition delay
NO	Nitrogen monoxide
NO_2	Nitrogen dioxide
NO_x	Nitric oxides
PM	Particulate matter
PMBF	Premixed burn fraction
RME	rapeseed methyl ester
SOC	Start of combustion
SOI	Start of injection
SN	Smoke number
THC	Total hydrocarbons
ULSD	Ultra-low sulfur diesel fuel

ACKNOWLEDGMETS

The experimental work of this research has been conducted in the Centre for Advanced Powertrain and Fuels Research (CAPF), School of Engineering and Design, Brunel University, London, UK. Authors are thankful to center staff and special thank is for technicians Kenneth Antiss, and to colleagues Fanos Christodoulou, David Peirce and N. Alozie for their assistance.

REFERENCES

1- Knothe, G.; Van Gerpen, J.; Krahl, J. The Biodiesel Handbook; AOCS Press: Champaign, IL, 2005.
2- C. Robbins, S.K. Hoekman, E. Ceniceros, M. Natarajan, Effects of biodiesel fuels upon criteria emissions, SAE International, SAE 2011-01-1943; JSAE 20119349,2011.
3- Glassman, I.; Yetter, R. A. Combustion, 4th ed.; Elsevier Academic Press: Burlington, MA, 2008.
4- Ban-Weiss, G. A.; Chen, J. Y.; Buchholz, B. A.; Dibble, R. W. A numerical investigation into the anomalous slight NOx increase when burning biodiesel; A new (old) theory. Fuel Process. Technol. 2007, 88, 659−667.
5- Turns, S. R. An Introduction to Combustion: Concepts and Applications, 2nd ed.; Tata McGraw-Hill: New Delhi, India, 2012.
6- D. M. Peirce, N. S. I. Alozie, D. W. Hatherill, and L. C. Ganippa . Premixed Burn Fraction: Its Relation to the Variation in NOx Emissions between Petro- and Biodiesel. Energy Fuels 2013, 27, 3838−3852.
7- S.K. Hoekman, A.W. Gertler, A. Broch, C. Robbins, M. Natarajan, Biodistillate transportation fuels 1. Production and properties. 2009-01-2766, SAE International. SAE Technical Paper Series, 2009.
8- S.K. Hoekman, A. Broch, C. Robbins, E. Ceniceros, M. Natarajan, Review of biodiesel composition, properties, and specfications, Renewable and Sustainable Energy Reviews 16 (2012) 143–169.
9- Bamgboye, A. I.; Hansen, A. C. Prediction of cetane number of biodiesel fuel from the fatty acid methyl ester (FAME) composition. Int. Agrophys. 2008, 22, 21−29.
21- Glaude, P. A.; Fournet, R.; Bounaceur, R.; Moliere, M. Adiabatic flame temperature from biofuels and fossil fuels and derived effect on NOx emissions. Fuel Process. Technol. 2010, 91, 229−235.
22- Pi-qiang Tan , Zhi-yuan Hu , Di-ming Lou a, Zhi-jun Li . Exhaust emissions from a light-duty diesel engine with Jatropha biodiesel fuel. Energy 39 (2012) 356- 362.
23- Yage Di , C.S. Cheung , Zuohua Huang . Experimental investigation on regulated and unregulated emissions of a diesel engine fueled with ultra-low sulfur diesel fuel blended with biodiesel from waste cooking oil. SCIENCE OF THE TOTAL ENVIRONMENT 407 (2009) 835 – 846.
10- Hellier, P.; Ladommatos, N.; Allan, R.; Payne, M.; Rogerson, J. The impact of saturated and unsaturated fuel molecules on diesel combustion and exhaust emissions. SAE Technical Paper 2011-01- 1922, 2011, 10.4271/2001-01-1922.
11- S. Kent Hoekman , Curtis Robbins. Review of the effects of biodiesel on NOx emissions. Fuel Processing Technology 96 (2012) 237–249.
12- J. Sun, J.A. Caton, T.J. Jacobs, Oxides of nitrogen emissions from biodiesel-fuelled diesel engines, Progress in Energy and Combustion Science 36 (2010) 677–695.
13- C.J. Mueller, A.L. Boehman, G.C. Martin, An experimental investigation of the origin of increased NOx emissions when fueling a heavy-duty compression ignition engine with soy biodiesel, SAE International, 2009-01-1792, 2009, pp. 1–28.
14- A.S. Cheng, A. Upatnieks, C.J. Mueller, Investigation of the impact of biodiesel fuelling on NOx emissions using an optical direct injection diesel engine, International Journal of Engine Research 7 (2006) 297–318.
15- J.P. Szybist, J. Song, M. Alam, A.L. Boehman, Biodiesel combustion, emissions and emission control, Fuel Processing Technology 88 (2007) 679–691.
16- J. Bittle, B. Knight, T. Jacobs, Interesting behavior of biodiesel ignition delay and combustion duration, Energy & Fuels 24 (2010) 4166–4177.
17- P. Ye, A.L. Boehman, Investigation of the impact of engine injection strategy on the biodiesel NOx effect with a common-rail turbocharged direct injection diesel engine, Energy & Fuels 24 (2010) 4215–4225.
18- Murphy, M. J.; Taylor, J. D.; McCormick, R. L. Compendium of Experimental Cetane Number Data; Report No. NREL/SR-540-36805; National Renewable Energy Laboratory: Golden, CO, 2004.
19- Vaughn, T.; Hammill, M.; Harris, M.; Marchese, A. J. Ignition delay of bio-ester fuel droplets. SAE Technical Paper 2006-01-3302, 2001, 10.4271/2006-01-3302.
20- Lapuerta M, Armas O, Jose RF. Effect of biodiesel fuels on diesel engine emissions. Prog Energy Combust 2008 ;34:198–223.
24- Ladommatos, N.; Rubenstein, P.; Bennett, P. Some effects of molecular structure of single hydrocarbons on sooting tendency. Fuel1996, 75, 114−124.
25- Eastwood, P. Particulate Emissions from Vehicles; John Wiley and Sons Ltd.: Chichester, U.K., 2008.
26- Neely, G.D., Sasaki, S., Huang, Y., Leet, J.A., Stewart, D.W., 2005. New Diesel Emission Control Strategy to Meet US Tier 2 Emissions Regulations. SAE Paper 2005-01-1091.
27- Musculus, M. P. B. On the correlation between NOx emissions and the diesel premixed burn. SAE Technical Paper 2004-01-1401, 2004, 104271/2004-01-1401.
28- Challen, B. & Baranescu, R. eds., 1999. Diesel Engine Reference Book. Second Edition, Butterworth-Heinemann: Oxford, UK.

29- Musculus, M. P. B. Measurements of the influence of soot radiation on in-cylinder temperatures and exhaust NOx in a heavy-duty DI diesel engine. SAE Technical Paper 2005-01-0925.
30- Guo, H.; Smallwood, G. J. The interaction between soot and NO formation in a laminar axisymmetric coflow ethylene/air diffusion flame. Combust. Flame 2007, 149, 225−233.
31- Ren, Y.; Li, X. Numerical simulation of the soot and NOx formations in a biodiesel-fuelled engine. SAE Technical Paper 2011- 01-1385.

ANNEX A

Summary of emissions results

Fuel type	load	Injection timing ATDC	NO_x ppm	NO ppm	NO_2 ppm	SN	CO ppm	THC ppm
ULSD	Low	-12	1930	1833	96	0.12	266	308
		-9	1571	1472	99	0.07	305	286
		-6	1238	1142	96	0.06	341	247
		-3	1040	938	99	0.05	408	261
		0	888	770	117	0.06	568	337
	High	-12	2587	2560	26	0.52	309	261
		-9	1931	1908	22	0.55	284	230
		-6	1407	1387	20	0.47	257	193
		-3	1075	1057	18	0.31	261	186
		0	910	868	16	0.2	269	180
RME	Low	-12	1790	1697	92	0.1	188	334
		-9	1412	1317	94	0.05	218	286
		-6	1146	1053	92	0.04	250	174
		-3	942	843	98	0.04	328	164
		0	796	679	117	0.05	534	196
	High	-12	2771	2730	40	0.48	315	310
		-9	2158	2121	36	0.38	288	260
		-6	1639	1609	29	0.31	261	225
		-3	1274	1247	27	0.21	269	245
		0	1058	1032	25	0.17	276	288